Cardiovascular Engineering and Technology, Vol. 10, No. 3, September 2019 *(© 2019)* pp. 397–422
https://doi.org/10.1007/s13239-019-00422-5

In-Vitro Pulsatile Flow Testing of Prosthetic Heart Valves: A Round-Robin Study by the ISO Cardiac Valves Working Group

Changfu Wu,[1] Neelakantan Saikrishnan,[2,13] Aaron J. Chalekian,[3] Rob Fraser,[4] Ornella Ieropoli,[5] Stephen M. Retta,[1] Russell Joseph,[6] Shouyan Lee,[7] Salvador Marquez,[6] David Mester,[8] Ning Pan,[9] Sepehr Vatanpour,[10] Craig Weinberg,[11] and Ulrich Steinseifer[12]

[1]Center for Devices and Radiological Health, Food and Drug Administration, Silver Spring, MD, USA; [2]Abbott, St. Paul, MN, USA; [3]Neovasc (U.S.) Inc, New Brighton, MN, USA; [4]ViVitro Labs, Victoria, BC, Canada; [5]Sorin Group Italia s.r.l. (fully owned by LivaNova Plc), Saluggia, VC, Italy; [6]Edwards Lifesciences LLC, Irvine, CA, USA; [7]Medical Implant Testing Lab, Irvine, CA, USA; [8]W. L. Gore & Associates, Inc., Flagstaff, AZ, USA; [9]Boston Scientific, Los Gatos, CA, USA; [10]Medtronic Inc, Minneapolis, MN, USA; [11]BDC Laboratories, Wheat Ridge, CO, USA; [12]RWTH-Aachen University, Aachen, Germany; and [13]Vdyne LLC, Maple Grove, MN, USA

(Received 23 February 2019; accepted 8 June 2019; published online 25 June 2019)

Associate Editor Ajit P. Yoganathan oversaw the review of this article.

Abstract

Purpose—Hydrodynamic performance testing is one of the core *in vitro* assessments required by the ISO 5840 series of standards for all prosthetic heart valves. A round-robin study carried out in 2005 in accordance with ISO 5840:2005 revealed significant variabilities in prosthetic heart valve hydrodynamic performance measurements among the participating laboratories. In order to re-examine the inter-laboratory variability based on the "state-of-the-art" under ISO 5840-1 and 5840-2:2015, the ISO Cardiac Valve Working Groups decided in 2016 to repeat the round-robin study.

Methods—A total of 13 international laboratories participated in the study. The test valves were chosen to be the St. Jude Medical Masters Series mechanical valves (19 mm aortic, 25 mm aortic, 25 mm mitral, and 31 mm mitral), which were circulated among the laboratories. The testing was conducted according to a common test run sequence, with prespecified flow conditions.

Results—The study revealed improved, yet still significant variability among different laboratories as compared to the 2005 study. The coefficient of variation ranged from 7.7 to 21.6% for the effective orifice area, from 10.1 to 32.8% for the total regurgitant fraction, and from 14.7 to 45.5% for the mean transvalvular pressure gradient.

Conclusions—The study revealed the ambiguities in the current versions of the ISO 5840 series of standards and the shortcomings of some participating laboratories. This information has allowed the ISO Working Group to incorporate additional clarifying language into the ISO 5840-1, -2, and -3 standards that are currently under revision to improve *in vitro* assessments. The results presented here can also be used by the testing laboratories to benchmark pulse duplicator systems and to train and certify testing personnel.

Keywords—Prosthetic heart valves, Hydrodynamic performance testing, Effective orifice area, Total regurgitant fraction, Mean pressure gradient, Waveform.

INTRODUCTION

Cardiac valves are hydraulic one-way valves performing the function of directing blood to pass through the four chambers of the heart in one direction. As such, the hydrodynamic design goals of a prosthetic heart valve are to maximize forward flow, minimize backward flow, and avoid flow-induced blood damage. The pulsatile forward and backward flow characteristics of a prosthetic heart valve are typically characterized *in vitro* using a pulse duplicator. International Organization for Standardization (ISO) standards 5840-2 and ISO 5840-3 define the size-dependent minimum hydrodynamic performance requirements (i.e., effective orifice area and regurgitant fraction) for surgical and transcatheter heart valve prostheses implanted in the left side of the heart, respectively.[5,6]

Pulsatile flow testing has long been considered the gold standard for characterizing hydrodynamic performance of prosthetic valves. This test method is expected to simulate clinically relevant flow conditions, while eliminating variations observed during hemody-

Address correspondence to Changfu Wu, Center for Devices and Radiological Health, Food and Drug Administration, Silver Spring, MD, USA. Electronic mail: Changfu.Wu@fda.hhs.gov

1869-408X/19/0900-0397/0 © 2019 This is a U.S. government work and its text is not subject to copyright protection in the United States; however, its text may be subject to foreign copyright protection

namic assessment of patients.[3,9,12] Pulsatile flow testing involves selection of various parameters that define the test conditions, including the beat rate, cardiac output, systolic duration and test pressure conditions. The ISO standards are prescriptive about the specific conditions to be utilized for pulsatile flow testing. In particular, testing at nominal conditions (70 beats/min, 5.0 L/min cardiac output, 35% systolic duration, normotensive conditions) is tied to the minimum performance criteria for prosthetic heart valves; all commercially approved prosthetic heart valves are expected to meet these minimum performance criteria.

However, the standards are less descriptive about the pulse duplicator and its waveforms, only stipulating that the pulse duplicator should produce pressure and flow waveforms that approximate physiological conditions over the required physiological range for testing. In practice, pulse duplicator designs vary significantly among the test laboratories. Some use commercial systems, and others use proprietary ones. These systems utilize a variety of design aspects, such as drive mechanism (e.g., pneumatic, piston driven), test chamber geometry (e.g., anatomically accurate, idealized tubes), compliance (e.g., fully rigid, lumped compliance element, fully compliant vasculature), and measurement instrumentation, which can result in significant variability in the waveforms utilized for testing. Since the prescribed conditions only consist of cycle-averaged and instantaneous hydrodynamic characteristics, the waveforms utilized by different test laboratories can differ significantly. In addition, given the lack of specificity in the test conditions with respect to waveforms, it is conceivable to "tune" a pulse duplicator system to obtain different input waveforms for the same test conditions—this severely affects the repeatability and reproducibility of this test method.[1,2,4,10] Variation in the waveforms used for testing has the potential to impact the performance measures obtained from pulsatile testing. This is in addition to any test method and operator variabilities, which could amplify differences in hydrodynamic performance results. Such variations in standardized performance metrics make it difficult to interpret the test results from both a regulatory and clinical standpoint. From a regulatory perspective, such variability diminishes the applicability and importance of a "gold standard" *in vitro* test, while from a clinical standpoint, it becomes difficult to objectively compare the performance measures provided for different prosthetic valves.

To evaluate the variability of the pulse duplicator testing for hydrodynamic performance measurement of prosthetic heart valves, four laboratories, including three heart valve manufacturers and the Food and Drug Administration, conducted an inter-laboratory comparison study in 2005, the results of which were published in 2017.[8] The round-robin study compared the transvalvular pressure drop and back flow leakage measured on one 25 mm bileaflet valve, monoleaflet valve, ball-and-cage valve, and pericardial tissue valve, respectively, in accordance with ISO 5840:2005. The results showed considerable variations among the participating laboratories. They were previewed prior to publication by ISO Technical Committee 150/Subcommittee 2/Working Group 1 (Cardiac Valves) during the working group meeting in Phoenix, AZ in January 2016. The working group members at the meeting determined that the prior results might no longer be relevant because the majority of the laboratories had developed or purchased more contemporary pulse duplicators subsequent to the previous study and the ISO standard had also been revised to the 2015 version (ISO 5840-1:2015 and ISO 5840-2:2015). The working group then decided to conduct a new round-robin study to examine the current state-of-the-art in measuring prosthetic heart valve pulsatile flow performance. In addition, a round-robin study may potentially provide reference data that can be utilized for better standardization of pulse duplicator testing. This paper summarizes the results of this round-robin study.

METHODS

Study Protocol

Thirteen laboratories took part in the round-robin study, including one academic laboratory (Helmholtz Institute of the RWTH University, Aachen, Germany), three testing service providers (BDC Laboratories, Wheat Ridge, CO; Medical Implant Testing Lab, Irvine, CA; ViVitro Laboratories, Victoria, British Columbia, Canada), eight heart valve manufacturers (Boston Scientific, Los Gatos, CA; Edwards Lifesciences, Surgical Heart Valve Therapy, Irvine CA; Edwards Lifesciences, Transcatheter Heart Valves, Irvine CA; Medtronic, Mounds View, MN; Neovasc, New Brighton, MN; Sorin Group Italia s.r.l. (fully owned by LivaNova Plc), Saluggia, Vercelli, Italy; St Jude Medical, St. Paul, MN; W. L. Gore, Flagstaff, AZ), and the Food and Drug Administration Office of Science and Engineering Laboratories (Silver Spring, MD). It was agreed upon that the laboratory names would be anonymized. The characteristics of the pulse duplicators used by the anonymized participating laboratories are shown in Table 1.

The test valves used were St. Jude Medical Masters Series mechanical valves of sizes 19 mm (model number 19AJ-501), 25 mm (model number 25AJ-501) and

TABLE 1. Characteristics of the pulse duplicators used by participating laboratories.

Laboratory	System	Aortic inflow geometry	Aortic outflow geometry	Mitral inflow geometry	Mitral outflow geometry	Heart valve chamber compliance
1	Proprietary	Anatomic ventricular model	Anatomic aortic root model with sinuses	Anatomic atrium simulation	Anatomic ventricular model	Compliant
2	Commercial	Straight tube	Straight tube	Straight tube	Straight tube	Rigid
3	Commercial	Anatomic ventricular model	Straight tube	Straight tube	Anatomic ventricular model	Rigid
4	Proprietary	Straight tube	Anatomic aortic root model with sinuses	Straight tube	Straight tube	Rigid
5	Proprietary	Anatomic ventricular model	Anatomic aortic root model with sinuses	Anatomic atrium simulation	Anatomic ventricular model	Rigid
6	Commercial	Anatomic ventricular model	Anatomic aortic root model with sinuses	Straight tube	Anatomic ventricular model	Compliant
7	Commercial	Anatomic ventricular model	Anatomic aortic root model with sinuses	Anatomic atrium simulation	Anatomic ventricular model	Compliant
8	Commercial	Anatomic ventricular model	Straight tube	Straight tube	Anatomic ventricular model	Rigid
9	Proprietary	Straight tube	Straight tube	Straight tube	Straight tube	Rigid
10	Proprietary	Straight tube	Straight tube	Straight tube	Straight tube	Rigid
11	Commercial	Straight tube	Straight tube	Straight tube	Straight tube	Rigid
12	Proprietary	Straight tube	Straight tube	Straight tube	Straight tube	Rigid
13	Commercial	Anatomic ventricular model	Anatomic aortic root model with sinuses	Straight tube	Anatomic ventricular model	Rigid

TABLE 2. Equivalent model numbers to test valves used in the round-robin study.

Position	Size (mm)	Model number
Aortic	19	19AJ-501; 19AECJ-50; 19ATJ-503
	25	25AJ-501; 25AECJ-502; 25ATJ-503
Mitral	25	25 MJ-501; 25MECJ-502; 25MTJ-503; 25METJ-504
	31	31 MJ-501; 31MECJ-502; 31MTJ-503; 31METJ-504

TABLE 3. Pre-specified test runs for hydrodynamic performance measurements.

Test runs	Beat rate (bpm)	Systolic duration (%)	Simulated cardiac output (LPM)	Mean aortic pressure (mmHg)
1	70	35	5	100
2	45	30	5	100
3	70	35	2	100
4	70	35	3.5	100
5	70	35	5	100
6	70	35	7	100
7	120	50	5	100
8	70	35	5	100

31 mm (model number 31MJ-501). The 19 and 25 mm valves were tested in the aortic position and the 25 and 31 mm valves were tested in the mitral position. These sizes were chosen to represent a small size and a nominal size valve for the aortic and mitral positions, respectively. The St. Jude Medical Masters Series mechanical valve model numbers represent different sewing cuff configurations. The pyrolytic carbon valve assembly is the same for all model numbers for a given size. Equivalent model numbers to test valves used in the round-robin study are listed in Table 2.

TABLE 4. Sampling frequencies and filter settings used by participating laboratories.

Laboratory	Sampling frequency (Hz)	Low-pass filter frequency (Hz)	
		Pressure	Flow
1	1000	40	40
2	5000	60	60
3	225	30	30
4	2048	30	30
5	2048	30	30
6	256 samples/beat	None	100
7	256 samples/beat	30	30
8	256 samples/beat	30	30
9	1000	30	30
10	100	30	30
11	5000	100	40
12	1000	30	30
13	256 samples/beat	30	30

All test valves were provided without the cuff, so each laboratory decided independently how to mount the valves in their pulse duplicator. The mechanical valves were chosen for the ease of handling and shipping, as well as better repeatability. A single set of test

TABLE 5. Clarified definitions for hydrodynamic performance measurement.

	Aortic position	Mitral position
Forward flow volume	Aortic flow between start of forward flow (1[a]) and end of forward flow (3)	Mitral flow between start of forward flow (1[b]) and end of forward flow (3)
Cardiac output	For *in vitro* testing, simulated cardiac output is used (forward aortic flow volume multiplied by beat rate; tolerance = ± 0.1 L)	For *in vitro* testing, simulated cardiac output is used (forward mitral flow volume multiplied by beat rate; tolerance = ± 0.1 L)
Start of systole (aortic)/diastole (mitral)	Beginning of forward aortic flow (i.e., zero crossing of flow to positive) (1)	Beginning of forward mitral flow (i.e., zero crossing of flow to positive) (1)
End of systole (aortic)/diastole (mitral)	End of forward aortic flow (i.e., zero crossing of flow to negative) (3)	End of forward mitral flow (i.e., zero crossing of flow to negative) (3)
Start of positive differential pressure	First crossing of aortic and ventricular waveforms (7)	First crossing of atrial and ventricular waveforms (7)
End of positive differential pressure	Second crossing of aortic and ventricular waveforms (i.e., the last crossing to negative just before the end of systole) (9). In general, the positive differential pressure period is 75–100% of the duration of systole	The last crossing to negative just before the end of diastole (9). In general, the positive differential pressure period is 75–100% of the duration of diastole
RMS calculation	Calculated over positive differential pressure period (7 to 9)	Same as Aortic (7 to 9)
Start of closure	End of forward aortic flow (i.e., zero crossing of aortic flow) (3)	End of forward mitral flow (i.e., zero crossing of mitral flow) (3)
End of closure	If no zero crossing of flow, use a linear extrapolation of highest slope of flow; if zero crossing, use the first zero crossing after the start of closure (5)	If no zero crossing of flow, use a linear extrapolation of highest slope of flow; if zero crossing, use the first zero crossing after the start of closure (5)
Start of leakage	End of closure (5)	Same as Aortic
End of leakage	Start of systole (1)	Start of diastole (1)
Total regurgitant volume	Aortic flow between start of closure (3) and end of leakage (1)	Mitral flow between start of closure (3) and end of leakage (1)
Mean pressure gradient	Time-averaged arithmetic mean value of pressure differential across valve (ventricular–aortic pressure) during positive differential pressure period (7 to 9)	Time-averaged arithmetic mean value of pressure differential across valve (atrial–ventricular pressure) during positive differential pressure period (7 to 9)

[a]Numbers 1–9 in the "Aortic position" column refer to time points shown in Fig. 1.
[b]Numbers 1–9 in the "Mitral position" column refer to time points shown in Fig. 2.

valves was circulated among the participating laboratories.

The test runs for hydrodynamic performance measurements were prespecified as in Table 3. These conditions are representative of the test conditions presented in the ISO standards for hydrodynamic testing. Runs 1, 5, and 8 were repeat test runs designed to examine intra-laboratory repeatability.

In addition, the study protocol stated the following: (1) the latest definitions of simulated cardiac output and effective orifice area (EOA) in accordance with ISO 5840-1:2015 would be used; (2) the filter settings (using ~ 30 Hz low-pass as a guideline) would be disclosed; and (3) the test medium would be saline at 37 °C. The sampling frequencies and filter settings used by the participating laboratories are listed in Table 4.

After the results of the first round of testing were compiled, significant variabilities were noted among the laboratories. The working group reviewed the results and believed that some of the variabilities were attributable to different definitions used in calculations. Thus, a list of clarified definitions was provided to each laboratory, as summarized in Table 5. Subsequently, some laboratories repeated the study.

The metrics calculated in this study are defined as follows:

$$EOA = \frac{q_{V_{RMS}}}{51.6\sqrt{\Delta P/\rho}}$$

$$\text{Total regurgitant fraction} = \frac{\text{Total regurgitant volume}}{\text{Forward flow volume}}.$$

Waveform Analysis

The participating laboratories were required to provide representative waveforms obtained during the nominal test condition (Run 5), in accordance with the requirements of the ISO 5840 standards. The wave-

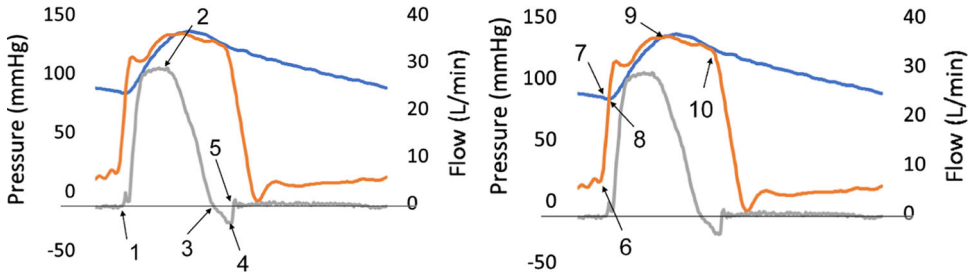

Attribute	Time points	Description of time points
1	Start forward flow	First zero crossing of flow curve in cycle
2	Peak forward flow	Peak flow
3	End forward flow	Second zero crossing of flow curve in cycle
4	Peak reverse flow	Minimum flow time point in cycle, occurring after end forward flow
5	End closing flow	If the flow crosses zero after peak reverse flow, this is the first zero crossing. If no zero crossing of flow occurs, a linear extrapolation of highest slope of flow is used.
6	Start ventricular contraction	Start of steep acceleration of ventricular pressure curve
7	Start positive differential pressure	First pressure crossing of ventricular and aortic pressures
8	Diastolic aortic pressure	Minimum aortic pressure time point
9	End positive differential pressure	Second pressure crossing of ventricular and aortic pressures
10	End ventricular contraction	Start of steep deceleration of ventricular pressure curve

FIGURE 1. Representative hydrodynamic waveforms for an aortic valve. Curves shown are ventricular pressure (orange), aortic pressure (blue) and aortic flow (gray). (a) Identified flow waveform attributes. (b) Identified pressure waveform attributes.

forms were analyzed both qualitatively and quantitatively. Qualitative analysis consisted of assessing overall characteristics of the flow and pressure waveforms, including acceleration, presence of steady/plateau regions, deceleration, inflexion points, minima, maxima, presence of high frequency oscillations and crossovers. These attributes are useful to identify general patterns of the flow and pressure waveforms. Quantitative analysis was conducted to identify the attributes shown in Figs. 1 and 2.

Key measures derived from the aortic waveforms are as follows:

- Flow acceleration period: Start forward flow (1) to peak forward flow (2)
- Forward flow period: Start forward flow (1) to end forward flow (3)
- Percent flow acceleration: Flow acceleration period divided by forward flow period
- Closing flow period: End forward flow (3) to end closing flow (5)
- Ventricular contraction period: Start ventricular contraction (6) to end ventricular contraction (10)
- Positive pressure differential period: Start positive differential pressure (7) to end positive differential pressure (9)
- Isovolumic contraction period: Start ventricular contraction (6) to start forward flow (1).

Key measures derived from the mitral waveforms are as follows:

- Flow acceleration period: Start forward flow (1) to peak forward flow (2)
- Forward flow period: Start forward flow (1) to end forward flow (3)
- Closing flow period: End forward flow (3) to end closing flow (5)
- Positive pressure differential period: Start positive differential pressure (7) to end positive differential pressure (9)

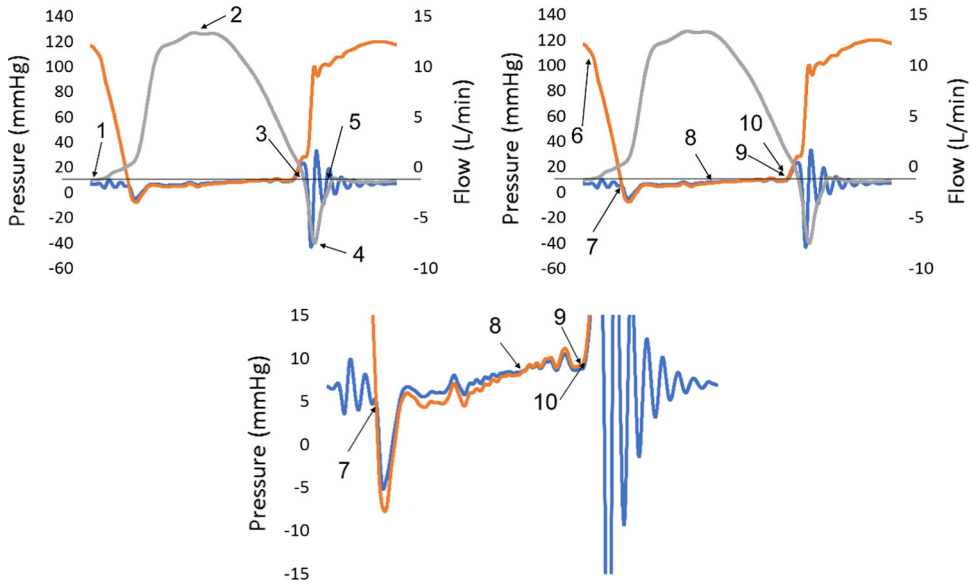

Attribute	Time points	Description of time points
1	Start forward flow	First zero crossing of flow curve in cycle
2	Peak forward flow	Peak flow
3	End forward flow	Second zero crossing of flow curve in cycle
4	Peak reverse flow	Minimum flow time point in cycle, occurring after end forward flow
5	End closing flow	If the flow crosses zero after peak reverse flow, this is the first zero crossing. If no zero crossing of flow occurs, a linear extrapolation of highest slope of flow is used.
6	End ventricular contraction	Start of steep deceleration of ventricular pressure curve
7	Start positive differential pressure	First pressure crossing of atrial and ventricular pressures
8	Second pressure crossing	Second pressure crossing of atrial and ventricular pressures
9	End positive differential pressure	Last pressure crossing of ventricular and aortic pressures
10	Start ventricular contraction	Start of steep acceleration of ventricular pressure curve

FIGURE 2. Representative hydrodynamic waveforms for a mitral valve. Curves shown are ventricular pressure (orange), atrial pressure (blue) and mitral flow (gray). (a) Identified flow waveform attributes. (b) Identified pressure waveform attributes. (c) Zoomed pressure waveforms to show crossings (7–10).

- Interim positive pressure differential period: Start positive differential pressure (7) to second pressure crossing (8)
- Ventricular relaxation period: End ventricular contraction (6) to start ventricular contraction (10)
- Isovolumic relaxation period: End ventricular contraction (6) to start forward flow (1)
- Percent flow acceleration: Flow acceleration period divided by forward flow period.

RESULTS

Hydrodynamic Performance

All laboratories used a uniform reporting template to report the results, including the pulse duplicator setup parameters, as prescribed in Table 3, and the measured valve hydrodynamic performances, such as EOA, total regurgitant fraction, and mean transvalvular pressure gradient. For laboratories that repeated the study, the results reported herein were from the second round of testing.

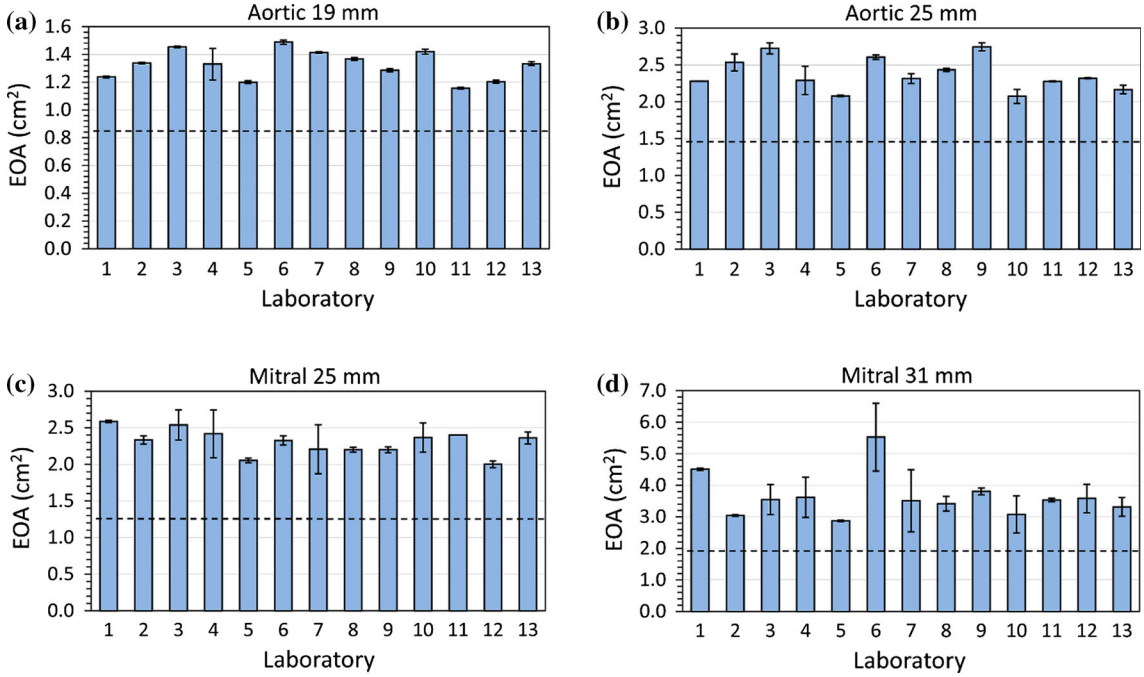

FIGURE 3. Measured effective orifice area. Dashed line represents minimum performance requirement for given valve size per ISO 5840-2:2015. Bar height and error bar represent the mean and standard deviation of Run 1, Run 5, and Run 8 results of a given laboratory, respectively.

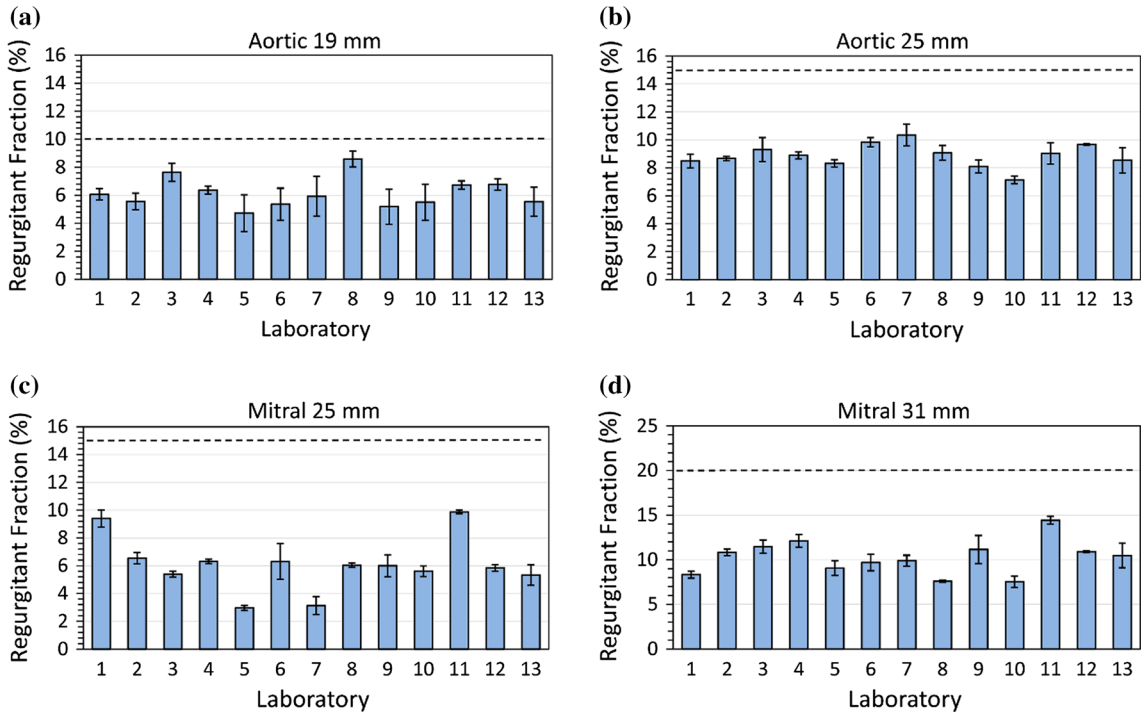

FIGURE 4. Measured total regurgitant fraction. Dashed line represents minimum performance requirement for a given valve size per ISO 5840-2:2015. Bar height and error bar represent the mean and standard deviation of Run 1, Run 5, and Run 8 results of a given laboratory, respectively.

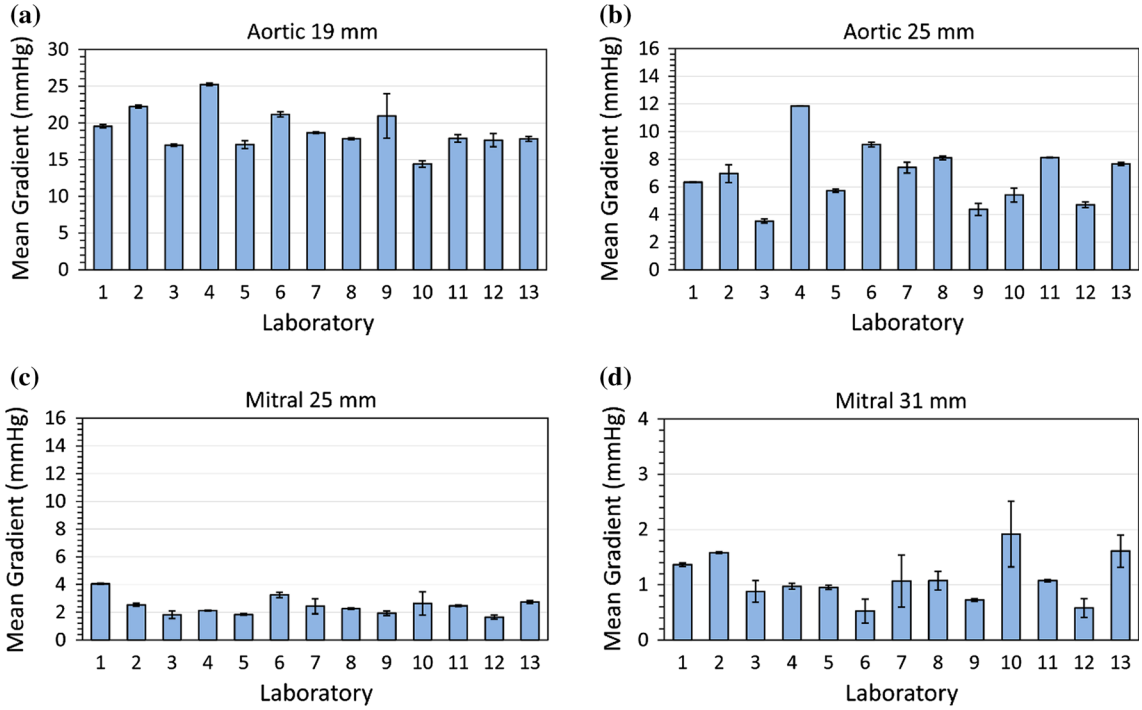

FIGURE 5. Measured mean pressure gradient. Bar height and error bar represent the mean and standard deviation of Run 1, Run 5, and Run 8 results of a given laboratory, respectively.

The measured pulsatile flow hydrodynamic performances under the nominal test condition (Runs 1, 5, and 8) are shown in Figs. 3, 4, and 5 for the EOA, total regurgitant fraction, and mean pressure gradient, respectively. The results presented represent the mean values averaged over Runs 1, 5, and 8. The hydrodynamic performance results for Runs 2, 3, 4, 6, and 7 are presented in Appendix A.

Most laboratories showed a reasonable intra-laboratory repeatability, as demonstrated by the standard deviations of the Runs 1, 5, and 8 results. The largest intra-laboratory standard deviation of the EOA was 1.1 cm^2 (Laboratory 6; 31 mm mitral valve; Fig. 3d), with a corresponding coefficient of variation of 19.5% and maximum peak-to-peak difference of 2.1 cm^2. Laboratory 9 had the largest intra-laboratory standard deviation for regurgitant fraction of 1.6% (31 mm mitral valve; Fig. 4d), with a corresponding coefficient of variation of 14.1% and maximum peak-to-peak difference of 3.1%. For the mean pressure gradient, the largest intra-laboratory standard deviation was 3.0 mmHg and was observed on the 19 mm aortic valve at Laboratory 9 (Fig. 5a); the corresponding coefficient of variation was 14.5% and maximum peak-to-peak difference was 5.4 mmHg.

The average EOAs measured by each laboratory under the nominal test conditions ranged from 1.2 to 1.5, 2.1 to 2.7, 2.0 to 2.6, and 2.9 to 5.5 cm^2 for the 19 mm aortic valve, 25 mm aortic valve, 25 mm mitral valve, and 31 mm mitral valve, respectively. The corresponding ranges of the average total regurgitant fraction were 4.7–8.6% (19 mm aortic), 7.1–10.4% (25 mm aortic), 3.0–9.9% (25 mm mitral), and 7.5–14.4% (31 mm mitral). The corresponding ranges of the average mean pressure gradient were 14.4 to 25.2 mmHg (19 mm aortic), 3.5 to 11.9 mmHg (25 mm aortic), 1.7 to 4.1 mmHg (25 mm mitral), and 0.5 to 1.9 mmHg (31 mm mitral). All EOA and total regurgitant fraction measurements met the minimum performance values of each test valve specified in ISO 5840-2:2015.

The summary results for each hydrodynamic performance parameter and test valve derived from the 39 test runs (13 laboratories with 3 test runs each) under the nominal test condition for all laboratories are shown in Table 6.

Waveforms Results

All the raw waveforms provided by the laboratories are presented in Appendix B, which were either individual waveforms or averaged over 10 cardiac cycles. Based on this round-robin study, it was discerned that the standard practices of reporting waveforms were different among the laboratories—some laboratories provided ensemble averaged waveforms, whereas others reported only individual cycle waveforms. The waveforms were highly variable in terms of the overall

TABLE 6. Hydrodynamic performance summary results under the nominal test condition.

	Summary Statistic[a]			
	Aortic 19 mm	Aortic 25 mm	Mitral 25 mm	Mitral 31 mm
EOA (cm^2)	1.3 ± 0.1 (1.2, 1.3, 1.5)	2.4 ± 0.2 (2.0, 2.3, 2.8)	2.3 ± 0.2 (1.9, 2.3, 2.7)	3.7 ± 0.8 (2.5, 3.6, 6.5)
Total regurgitant fraction (%)	6.1 ± 1.3 (3.8, 6.2, 9.1)	8.9 ± 0.9 (6.8, 8.8, 11.1)	6.1 ± 2.0 (2.7, 5.9, 10.0)	10.3 ± 2.0 (6.8, 10.6, 14.8)
Closing fraction	1.8 ± 0.8 (0.8, 1.6, 3.8)	5.1 ± 1.2 (3.2, 5.1, 7.3)	3.8 ± 1.0 (2.5, 3.5, 5.6)	6.7 ± 1.8 (3.7, 6.4, 10.4)
Leakage fraction	4.6 ± 1.1 (2.4, 4.7, 6.7)	3.9 ± 1.0 (1.7, 3.9, 5.7)	2.4 ± 1.3 (0.0, 2.5, 4.9)	3.6 ± 1.7 (0.0, 3.4, 6.9)
Mean pressure gradient (mmHg)	19.0 ± 2.8 (14.0, 18.5, 25.4)	6.9 ± 2.2 (3.4, 4.9, 11.9)	2.4 ± 0.7 (1.5, 2.3, 4.1)	1.1 ± 0.5 (0.3, 1.0, 2.4)

[a]Mean ± SD (minimum, median, maximum).

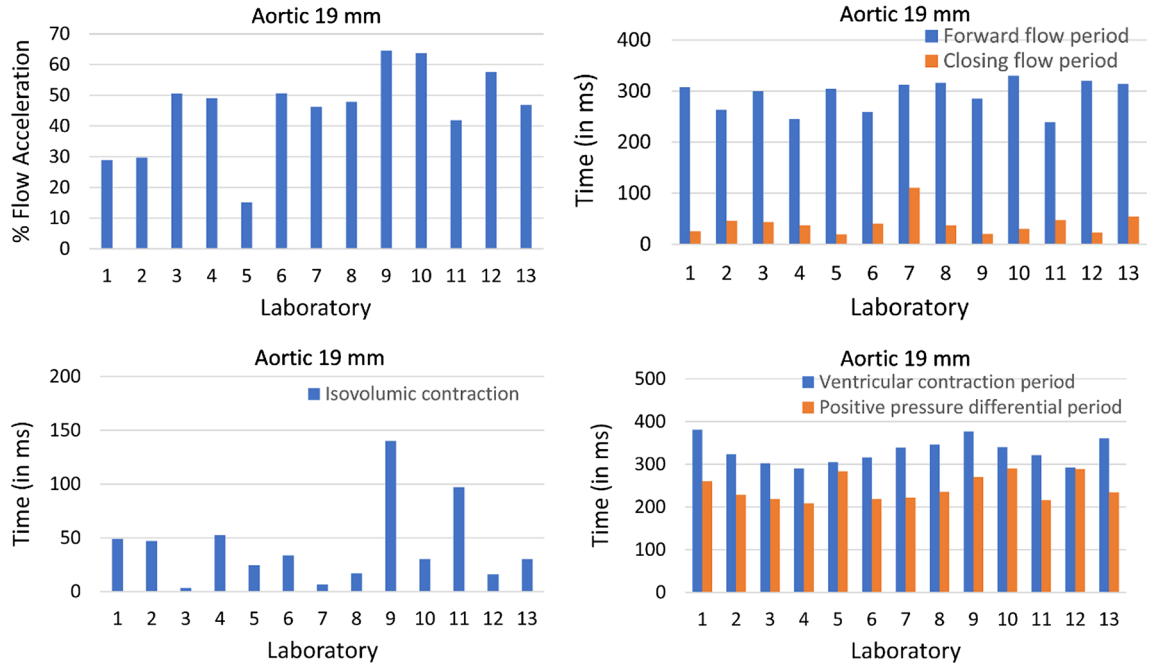

FIGURE 6. Quantitative measurements from the 19 mm aortic valve waveforms.

characteristics of the flow and pressure. In the aortic waveforms, most laboratories showed a sharp early systolic acceleration of ventricular pressure, which corresponded with an increase in the flow rate through the valve. Aortic pressures were nominally lowest prior to valve opening, with peak aortic pressures achieved after peak flow rate. Most laboratories showed a distinct closing phase of the flow waveform, prior to the leakage phase; some of the waveforms displayed high frequency oscillations (e.g., Laboratories 5, 10, 11, and 12 in Fig. B.1); and two laboratories showed plateau shaped flow and pressure waveforms (e.g., Laboratories 5 and 12 in Fig. B.1).

Quantitative assessments for the various valve configurations are presented in Figs. 6, 7, 8, and 9. The summary statistics are presented in Tables 7 and 8. Significant variability existed in the various metrics assessed across the different laboratories.

DISCUSSION

The 2005 round-robin study included a 25 mm St Jude Medical bileaflet aortic valve.[8] Thus, it is possible to compare the 2005 results with the current study (2016 study). Table 9 is a side-by-side comparison of

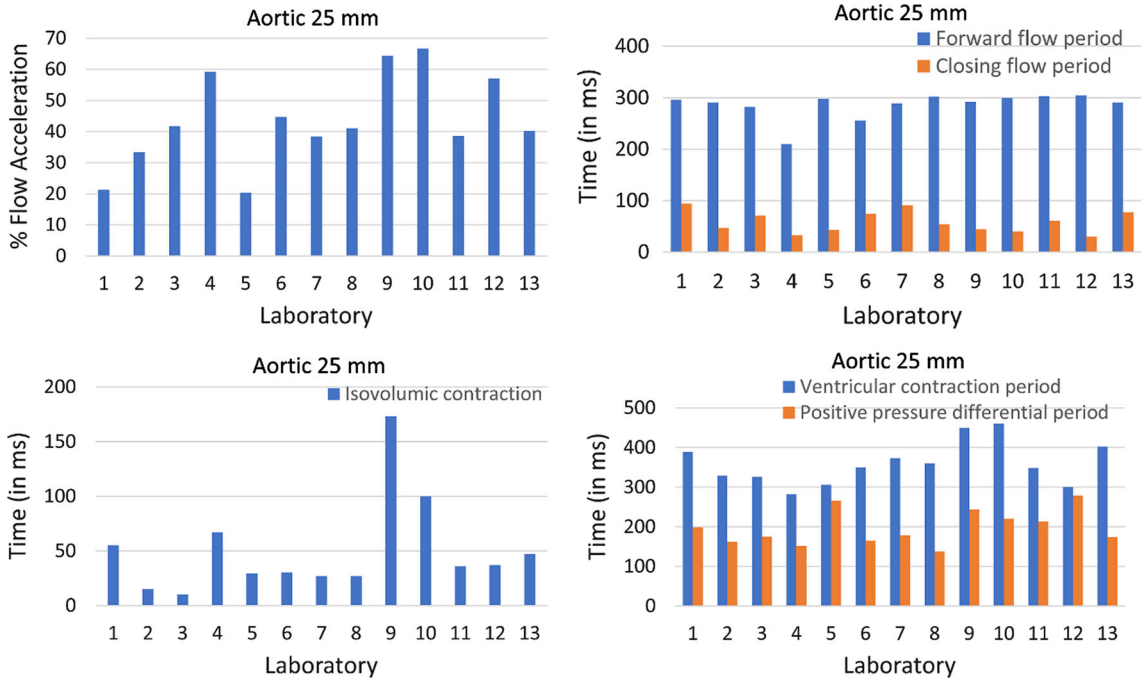

FIGURE 7. Quantitative measurements from the 25 mm aortic valve waveforms.

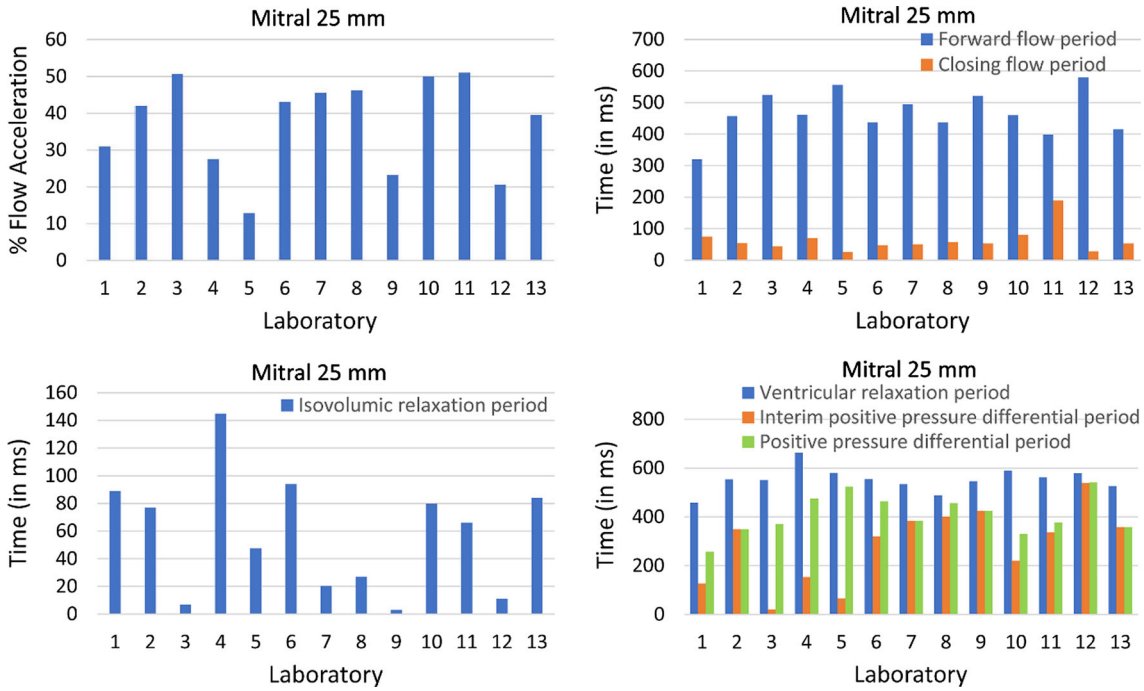

FIGURE 8. Quantitative measurements from the 25 mm mitral valve waveforms.

the hydrodynamic performance metrics measured under the nominal test conditions between the two studies. The current study consistently had smaller coefficients of variation, which indicates smaller variabilities in the current measurements.

Despite that the current round-robin study presented less variable results than the 2005 study, significant variability remains in some cases. For the four valves tested, the coefficient of variation ranged from 7.7 to 21.6% for the EOAs, from 10.1 to 32.8% for the

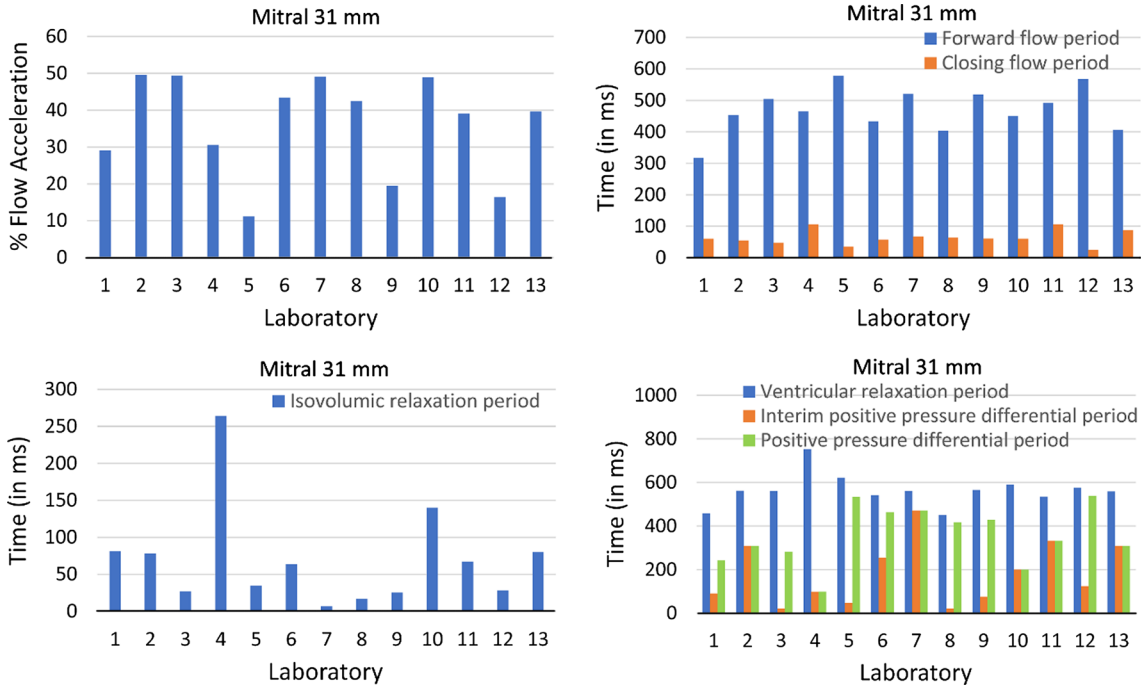

FIGURE 9. Quantitative measurements from the 31 mm mitral valve waveforms.

TABLE 7. Summary statistics of quantitative waveform parameters—aortic valves.

	Summary statistic[a]	
Parameters	19 mm Aortic	25 mm Aortic
Percent flow acceleration (%)	46 ± 14 (15, 48, 65)	44 ± 15 (20, 41, 67)
Forward flow period (ms)	292 ± 30 (239, 304, 330)	286 ± 26 (210, 292, 305)
Closing flow period (ms)	41 ± 24 (19, 37, 111)	58 ± 21 (30, 54, 91)
Isovolumic contraction period (ms)	42 ± 38 (3, 30, 140)	50 ± 44 (10, 36, 173)
Ventricular contraction period (ms)	330 ± 30 (290, 323, 377)	359 ± 54 (282, 349, 460)
Positive pressure differential period (ms)	244 ± 30 (208, 234, 290)	197 ± 44 (168, 178, 279)

[a]Mean ± SD (minimum, median, maximum).

total regurgitant fractions, and from 14.7 to 45.5% for the mean pressure gradients. The sources of the variabilities were multifactorial, such as the tester design (e.g., where the flow meters and pressure transducers were mounted, geometries of the inflow and outflow chambers, and drive mechanism—piston vs. pneumatic), the waveform shape, and data processing (e.g., filtering parameters, transducer calibration, system tuning, and selection of data points for calculations).

As shown in Table 1, significant variations existed among the pulse duplicator systems used for the round-robin study, including the use of rigid vs. compliant valve chambers, as well as anatomic vs. non-anatomic inflow and outflow geometries. In comparison to physiological waveforms, some laboratories displayed more conformance to clinically expected waveform characteristics as shown in Figs. 1 and 2 in ISO 5840-1:2015 than did others. For convenience, the Wiggers diagram shown in Fig. 2 in ISO 5840-1:2015 is recreated in Fig. 10, which shows expected physiological pressure waveforms and the corresponding flow waveforms, where the flow waveforms exhibit a steep initial flow acceleration, followed by a reduction in ventricular filling rate. Two laboratories showed pla-

TABLE 8. Summary statistics of quantitative waveform parameters—mitral valves.

	Summary statistic[a]	
Parameters	25 mm Mitral	31 mm Mitral
Percent flow acceleration (%)	37 ± 13 (13, 42, 51)	36 ± 13 (11, 40, 50)
Forward flow period (ms)	466 ± 70 (320, 460, 580)	470 ± 72 (317, 465, 578)
Closing flow period (ms)	63 ± 41 (26, 53, 189)	64 ± 24 (25, 60, 106)
Positive pressure differential period (ms)	408 ± 81 (257, 383, 541)	356 ± 133 (98, 332, 538)
Interim positive pressure differential period (ms)	284 ± 154 (20, 336, 539)	181 ± 143 (20, 124, 470)
Ventricular relaxation period (ms)	553 ± 50 (457, 554, 663)	564 ± 74 (450, 561, 753)
Isovolumic relaxation period (ms)	58 ± 43 (3, 66, 145)	70 ± 69 (7, 64, 264)

[a]Mean ± SD (minimum, median, maximum).

TABLE 9. Comparison in measured hydrodynamic performances between the 2005 study and the 2016 study.

	2005 Study		2016 Study	
	Mean ± SD	CV (%)	Mean ± SD	CV (%)
EOA (cm^2)	2.7 ± 0.3	11.1	2.4 ± 0.2	8.3
Total regurgitant fraction (%)	9.0 ± 3.0	33.3	8.9 ± 0.9	10.1
Mean pressure gradient (mmHg)	5.0 ± 2.8	56.0	6.9 ± 2.2	31.9

SD Standard deviation, *CV* coefficient of variation.

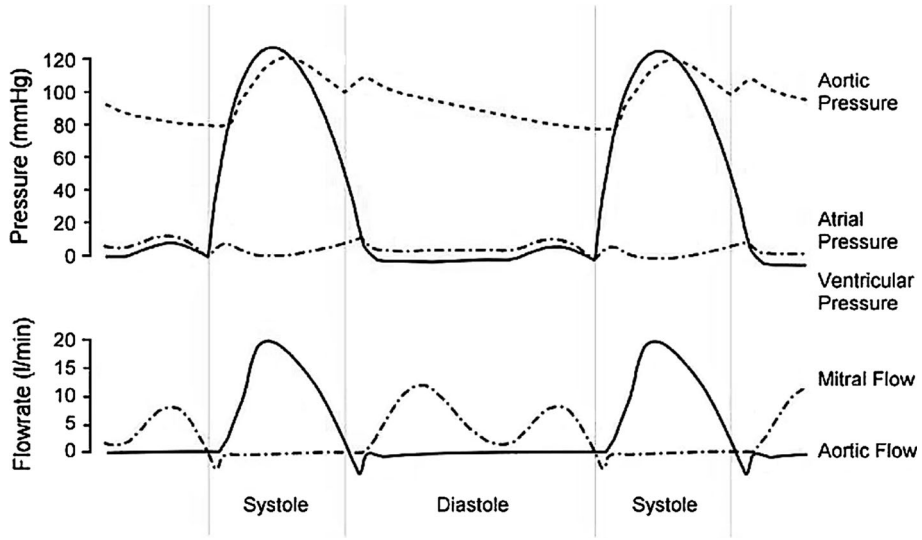

FIGURE 10. Wiggers Diagram, showing various events of a cardiac cycle (recreated with permission from ISO 5840-1:2015).

teau shaped flow and pressure waveforms, which might be related to specific system design. However, there were no broad similarities among flow waveforms from similar systems, suggesting that system tuning may have a more significant role in the waveforms shapes and characteristics. In addition, some of the waveforms displayed high frequency oscillations, potentially relating to filtering methods; however, some of these

oscillations might also be unique to testing mechanical heart valves due to the rapid closure of the rigid mechanical valve leaflets that do not provide any damping of the oscillations, which may not be observed in testing bioprosthetic valves.

Differences observed in the quantitative waveform parameters reflected the qualitative variations in the waveforms. However, the exact relationship between variations in the waveforms to the differences in the valve hydrodynamic performance measures cannot be determined through this exercise due to the complicated relationship between various flow and pressure parameters that determine the valve hydrodynamic performance measures.

Despite the variations seen in EOA and total regurgitant fraction, the results from all participating laboratories met the minimum performance criteria for EOA and total regurgitant fraction specified in ISO 5840-2:2015. This result might have led some laboratories to place less emphasis on the details of the testing, such as assessment of the physiological relevance of the waveforms and evaluation of the validity of the measurements; the first-round results from some laboratories contained human errors (e.g., inadequate sealing between the valve housing and the mounting fixture leading to erroneous total regurgitant fraction measurements). Nevertheless, it is important to note that the relative "insensitivity" in meeting the minimum hydrodynamic performance requirements to waveform characteristics, as shown in the current study, might not be extrapolatable to other prosthetic heart valve types because mechanical heart valves have shown extensive history of meeting the minimum performance criteria. Therefore, in order to obtain valid and physiologic measurements of valve hydrodynamic performance, it is important to properly tune the pulse duplicator system to not only achieve the operating flow parameters (i.e., beat rate, systolic duration, simulated cardiac output, and mean aortic pressure), but also generate a physiologically relevant waveform. In addition, as opposed to the more global valve performance measures such as EOA and total regurgitant fraction, the differences in waveform characteristics may have a greater impact on more detailed characterization of local flow characteristics as assessed using techniques such as particle image velocimetry (PIV) and computational fluid dynamics (CFD).[7,11]

CONCLUSION

The purpose of this round-robin study was to examine the inter-laboratory variability based on the "state-of-the-art" in prosthetic heart valve hydrodynamic performance measurements. The study revealed improved reproducibility when compared to a previous round-robin study, yet significant variability among different laboratories still exists. It also revealed that prosthetic heart valve hydrodynamic performance testing involves not only "science," but also "art," especially in the tuning of flow and pressure waveforms. The variabilities observed were partly inherent to the testing methodology; however, it is not practical to standardize the tester design and waveform shapes. Therefore, it is important to exercise care in the testing by carefully tuning the pulse duplicator system in order to minimize the variations and obtain valid and repeatable measurements. This information has allowed the ISO Working Group to incorporate improved language into the ISO 5840-1, -2, and -3 standards that are currently under revision. The results presented here can also be used by the testing laboratories to benchmark pulse duplicator systems, as well as to train and certify testing personnel.

APPENDIX A

Appendix A contains the valve hydrodynamic performance results for Runs 2, 3, 4, 6, and 7.

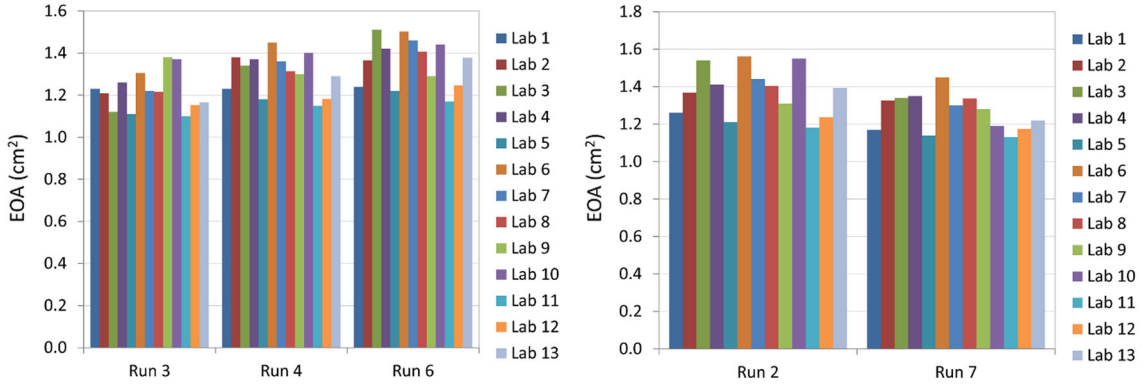

(a) Effective orifice area

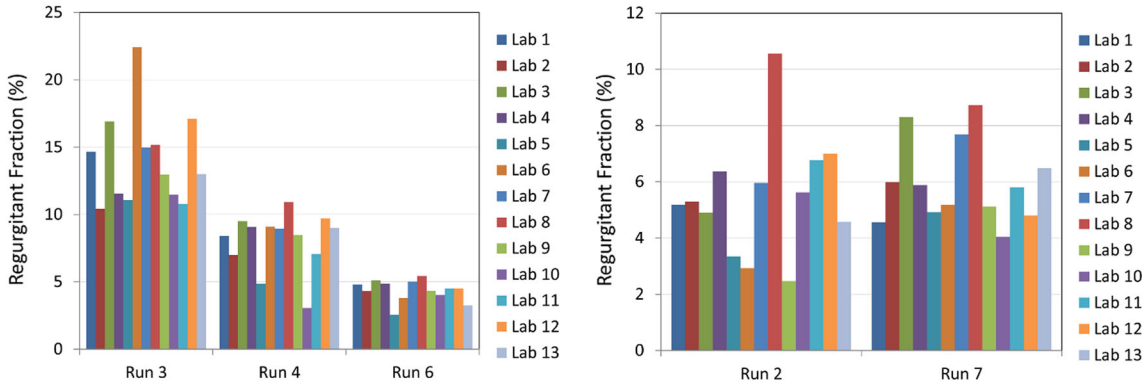

(b) Total regurgitant fraction

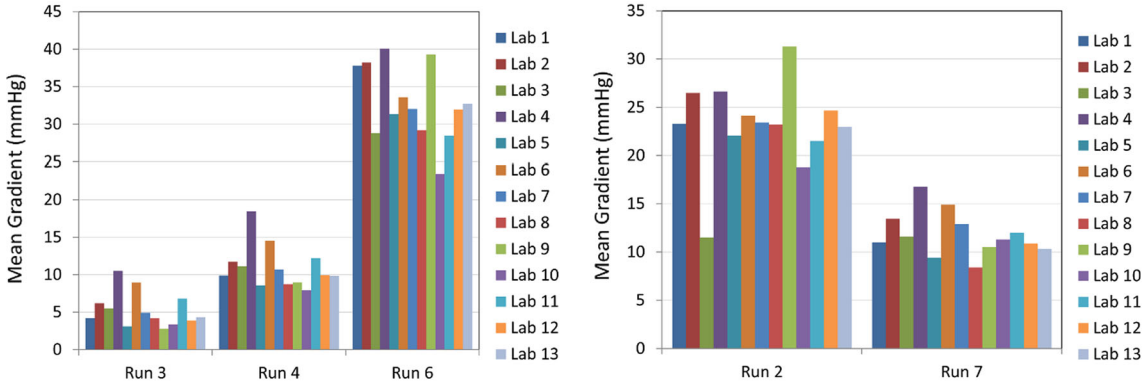

(c) Mean pressure gradient

FIGURE A.1. Valve hydrodynamic performances—19 mm aortic (Runs 2, 3, 4, 6, and 7).

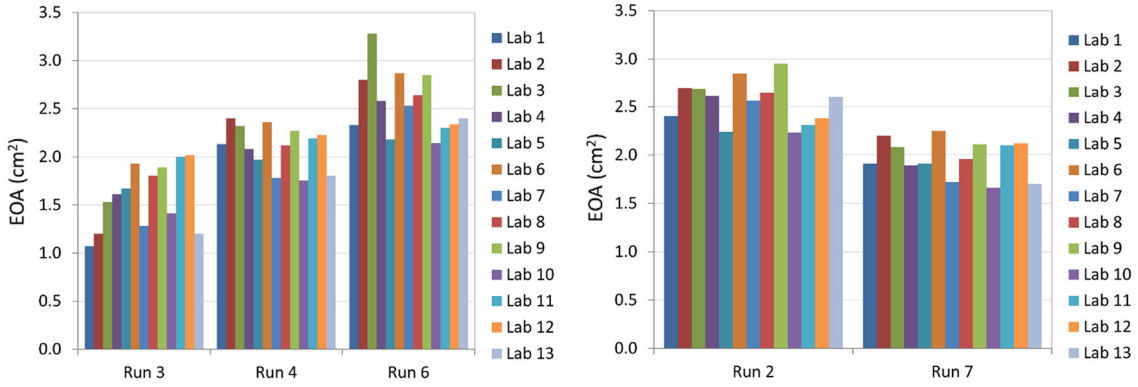

(a) Effective orifice area

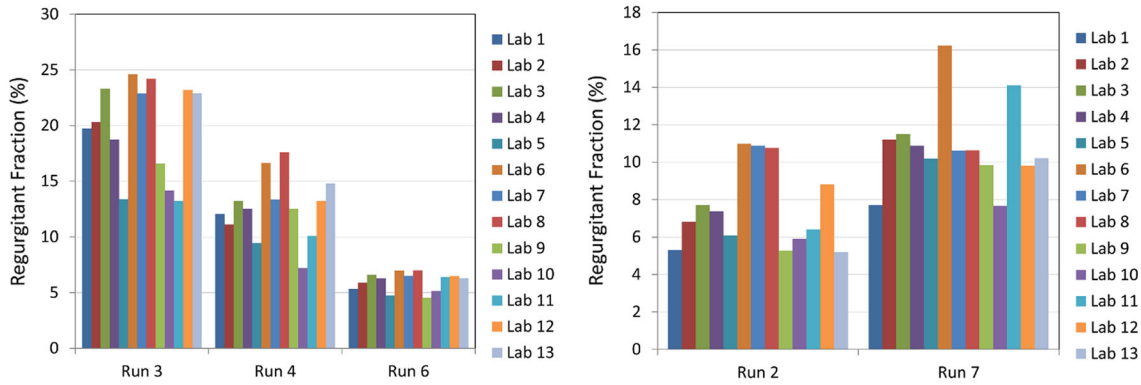

(b) Total regurgitant fraction

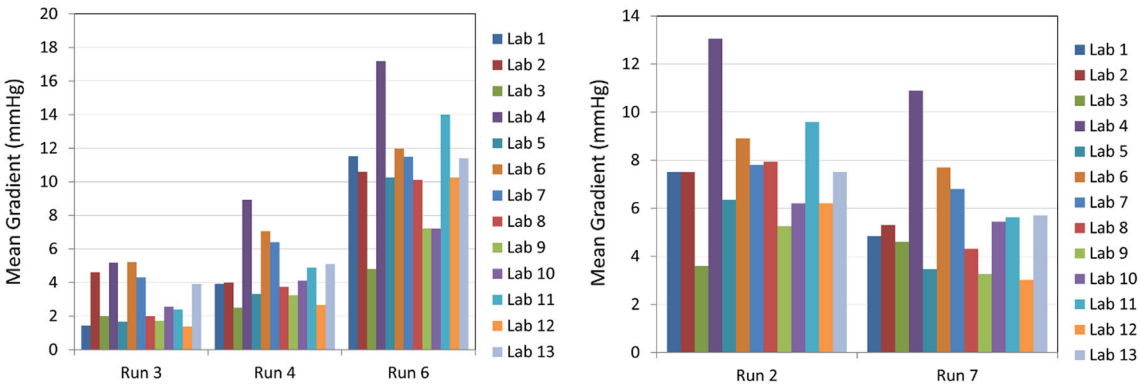

(c) Mean pressure gradient

FIGURE A.2. Valve hydrodynamic performances—aortic 25 mm (Runs 2, 3, 4, 6, and 7).

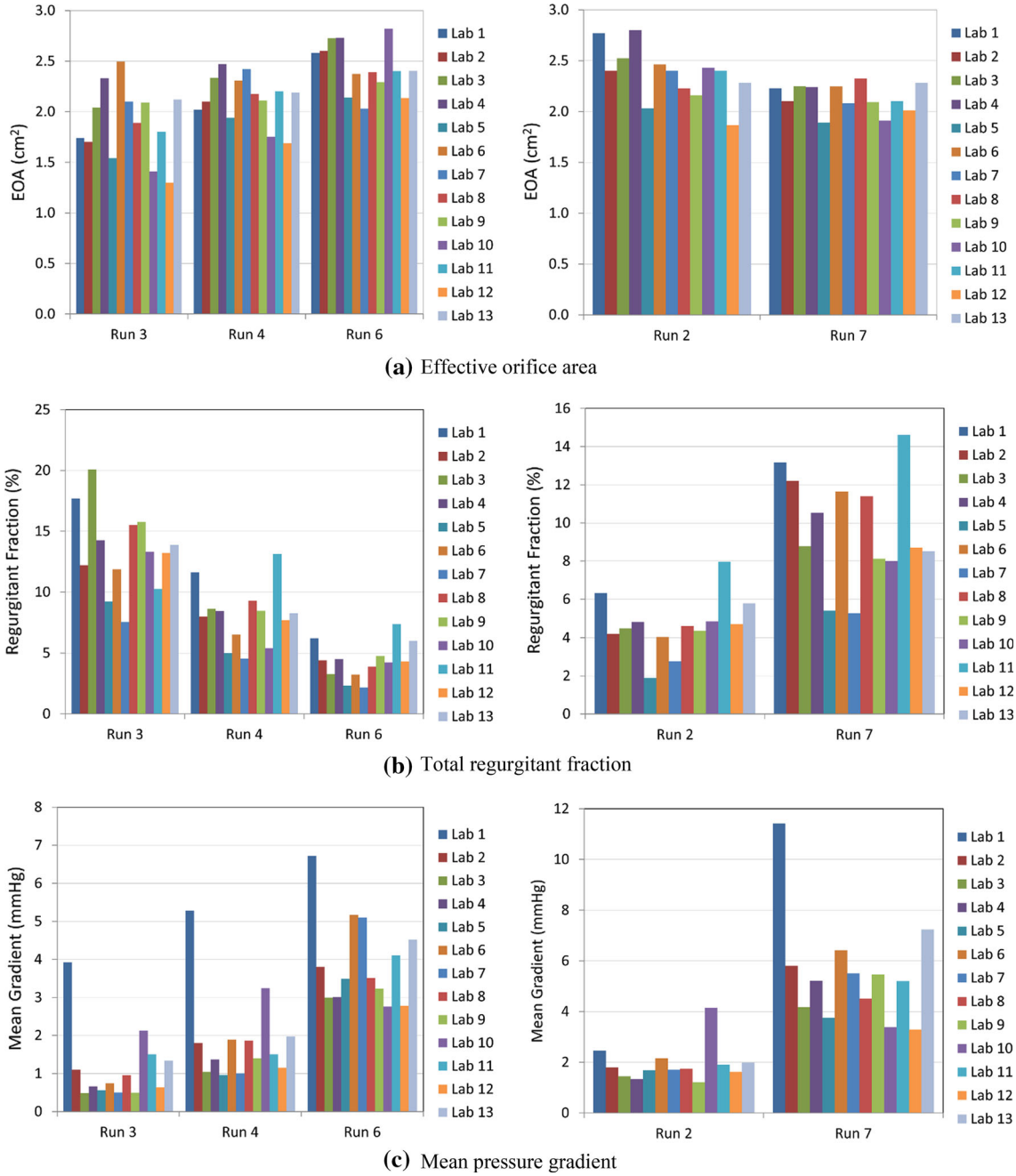

FIGURE A.3. Valve hydrodynamic performances—mitral 25 mm (Runs 2, 3, 4, 6, and 7).

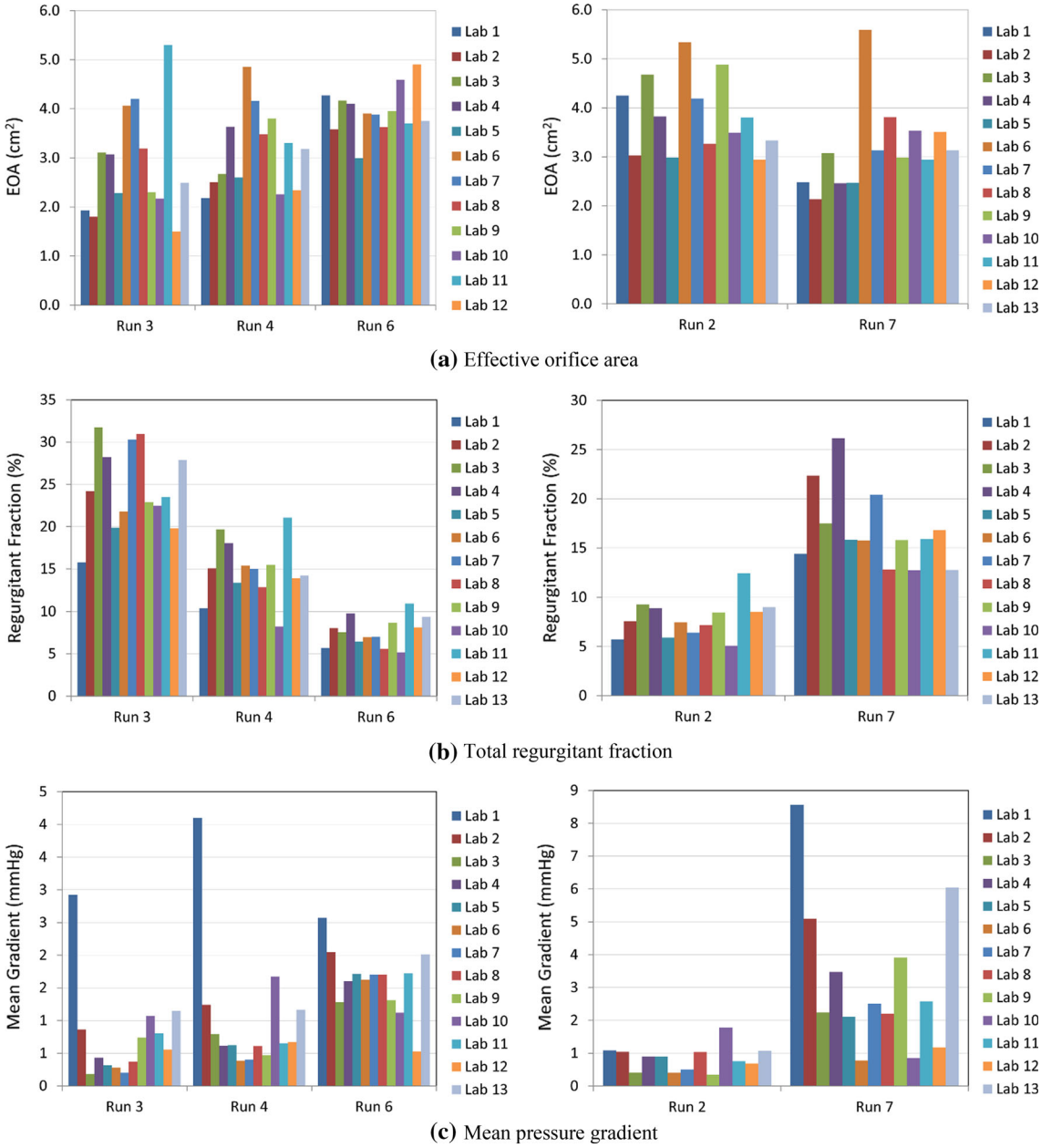

(a) Effective orifice area

(b) Total regurgitant fraction

(c) Mean pressure gradient

FIGURE A.4. Valve hydrodynamic performances—mitral 31 mm (Runs 2, 3, 4, 6, and 7).

APPENDIX B

Appendix B contains the raw hydrodynamic waveforms obtained from the different laboratories.

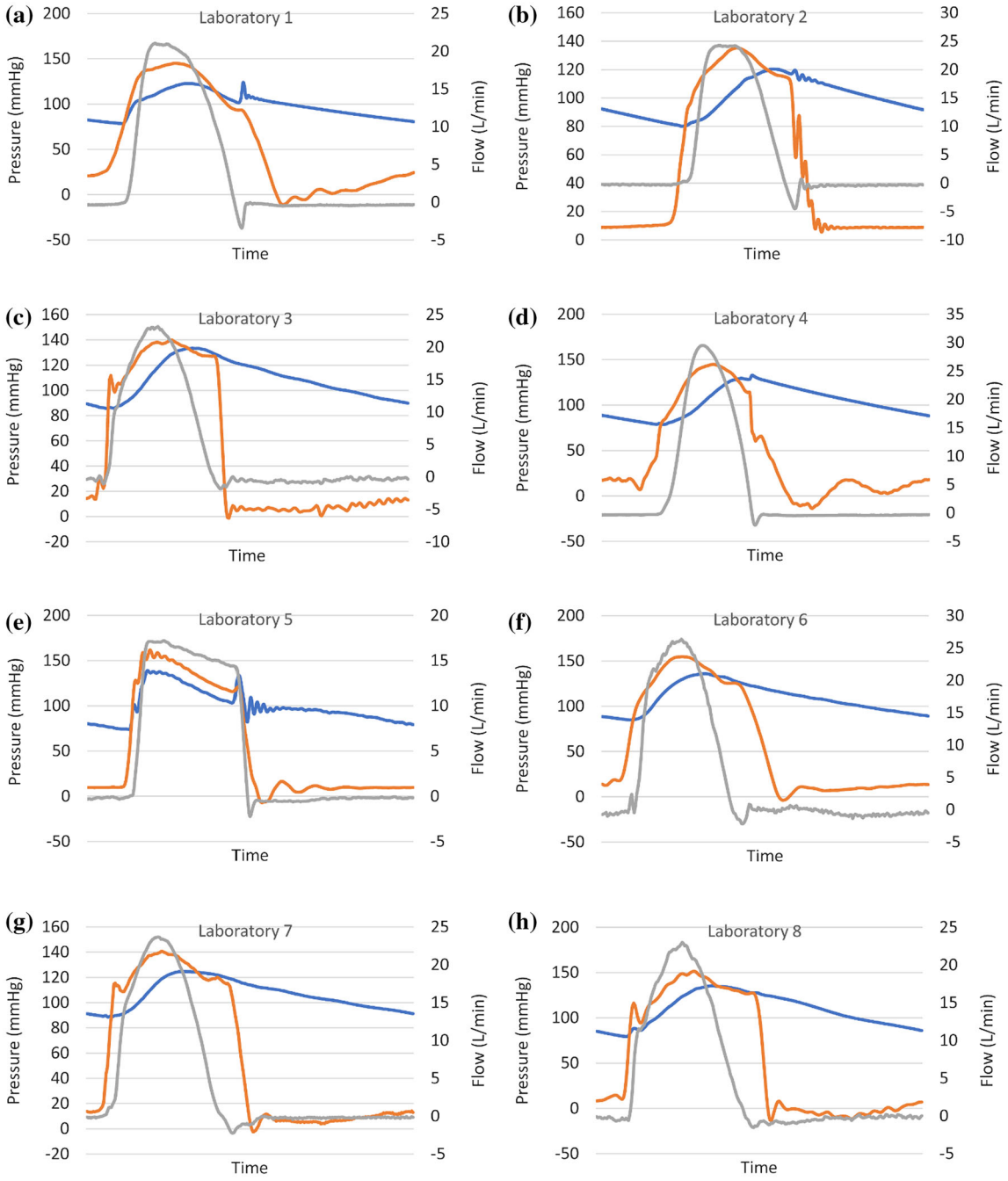

FIGURE B.1. Pressure and flow waveforms - aortic 19 mm. Curves shown are ventricular pressure (orange), aortic pressure (blue) and aortic flow (gray).

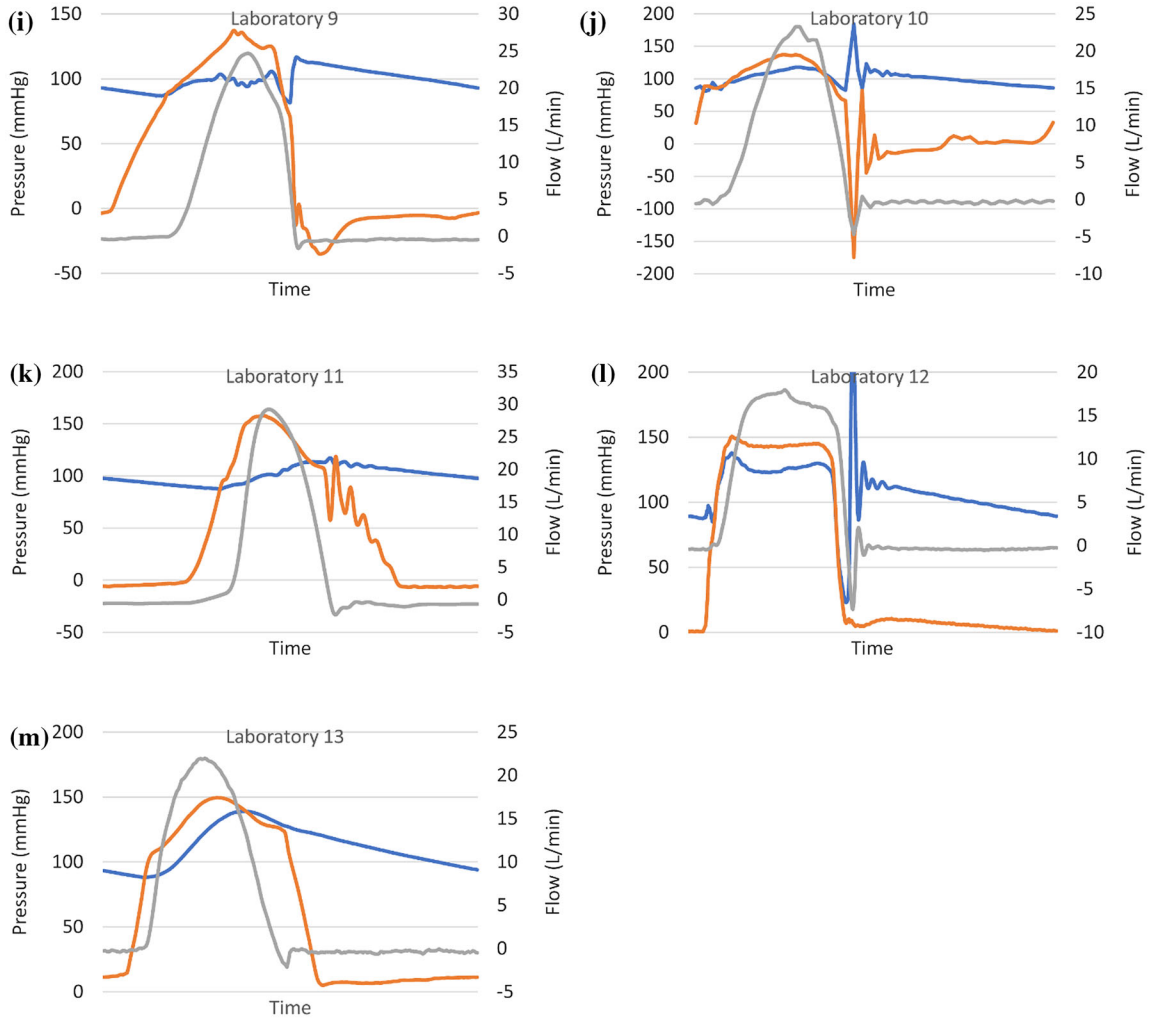

FIGURE B.1. continued

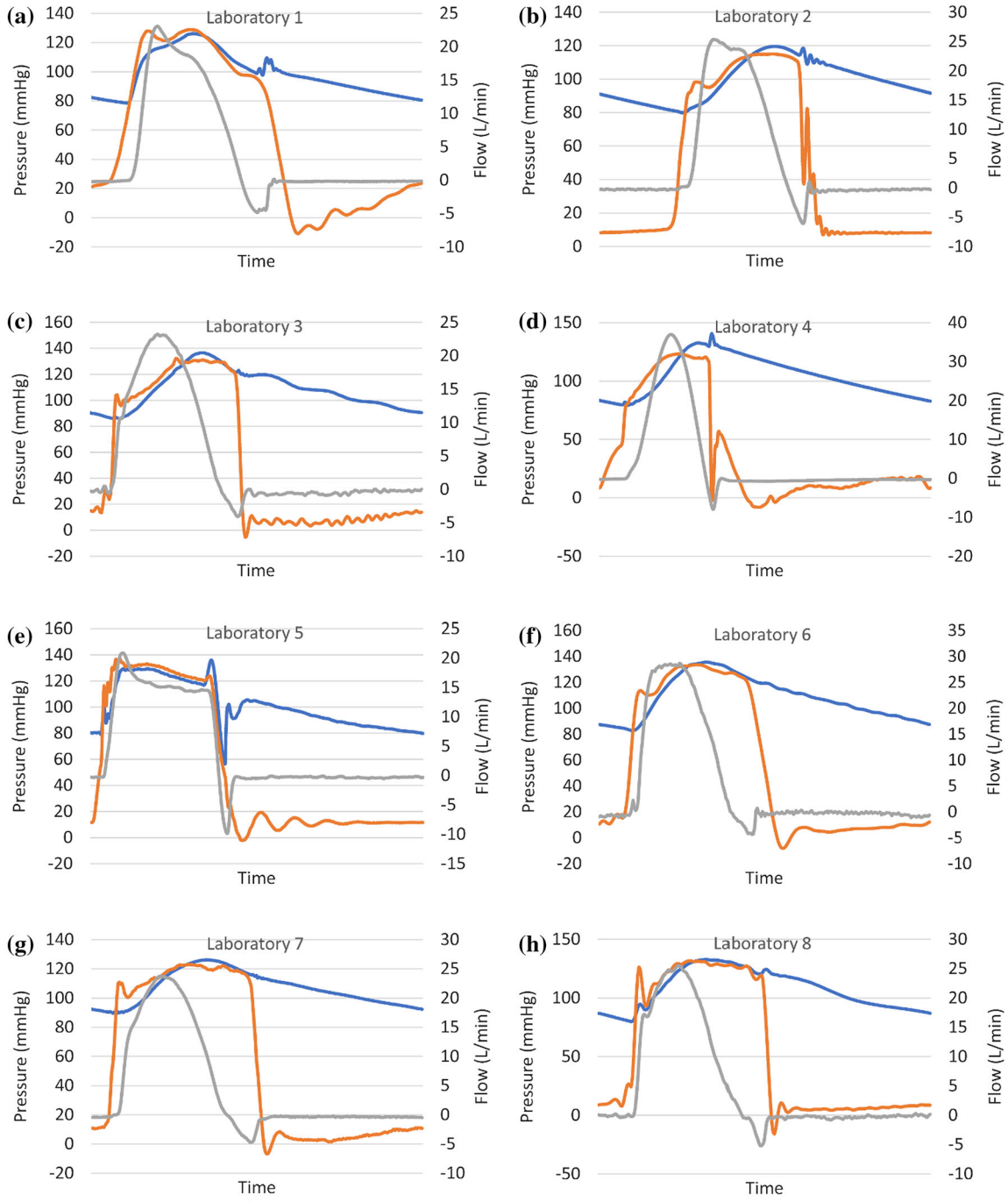

FIGURE B.2. Pressure and flow waveforms - 25 mm aortic. Curves shown are ventricular pressure (orange), aortic pressure (blue) and aortic flow (gray).

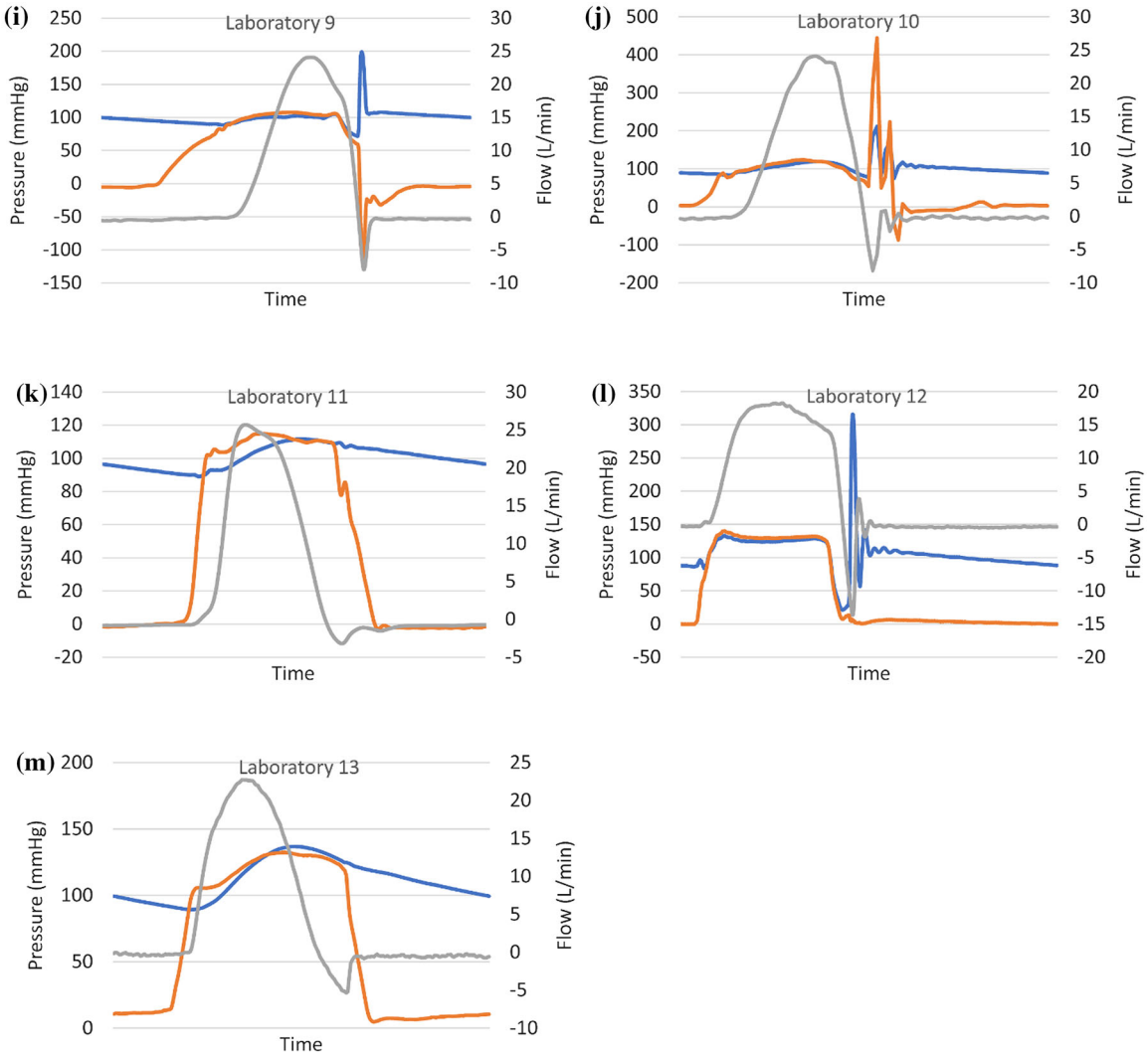

FIGURE B.2. continued

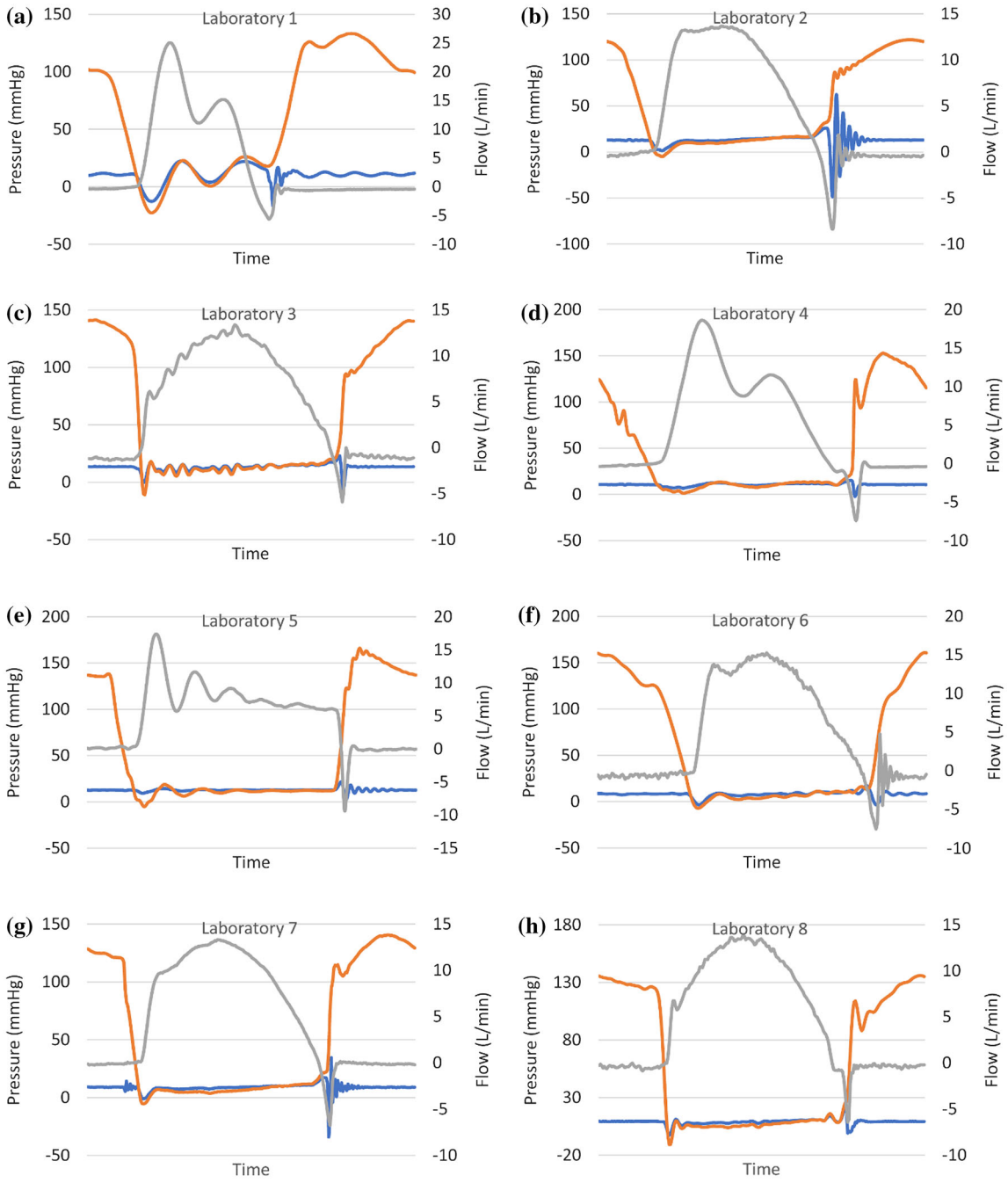

FIGURE B.3. Pressure and flow waveforms—mitral 25 mm. Curves shown are ventricular pressure (orange), atrial pressure (blue) and mitral flow (gray).

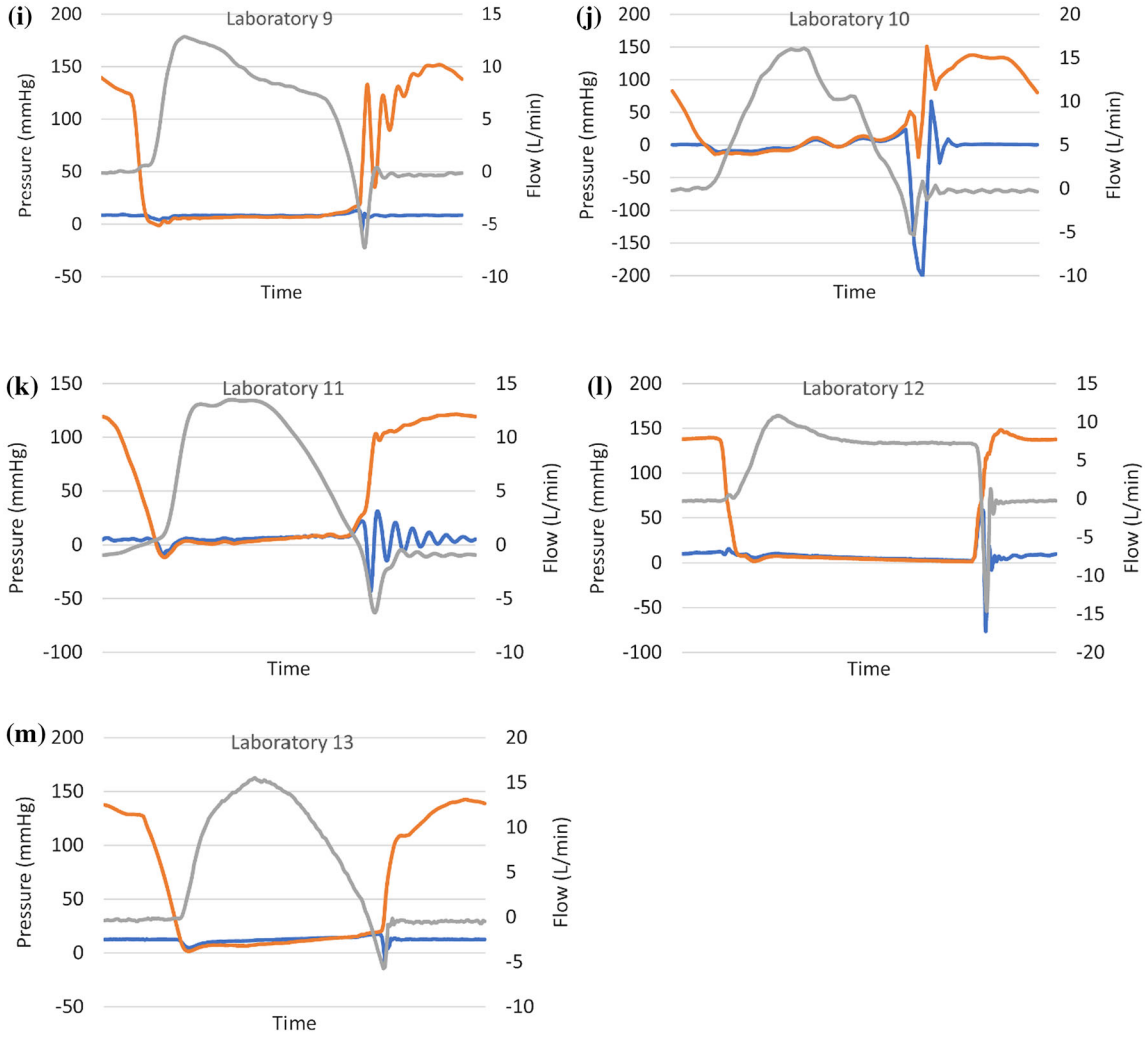

FIGURE B.3. continued

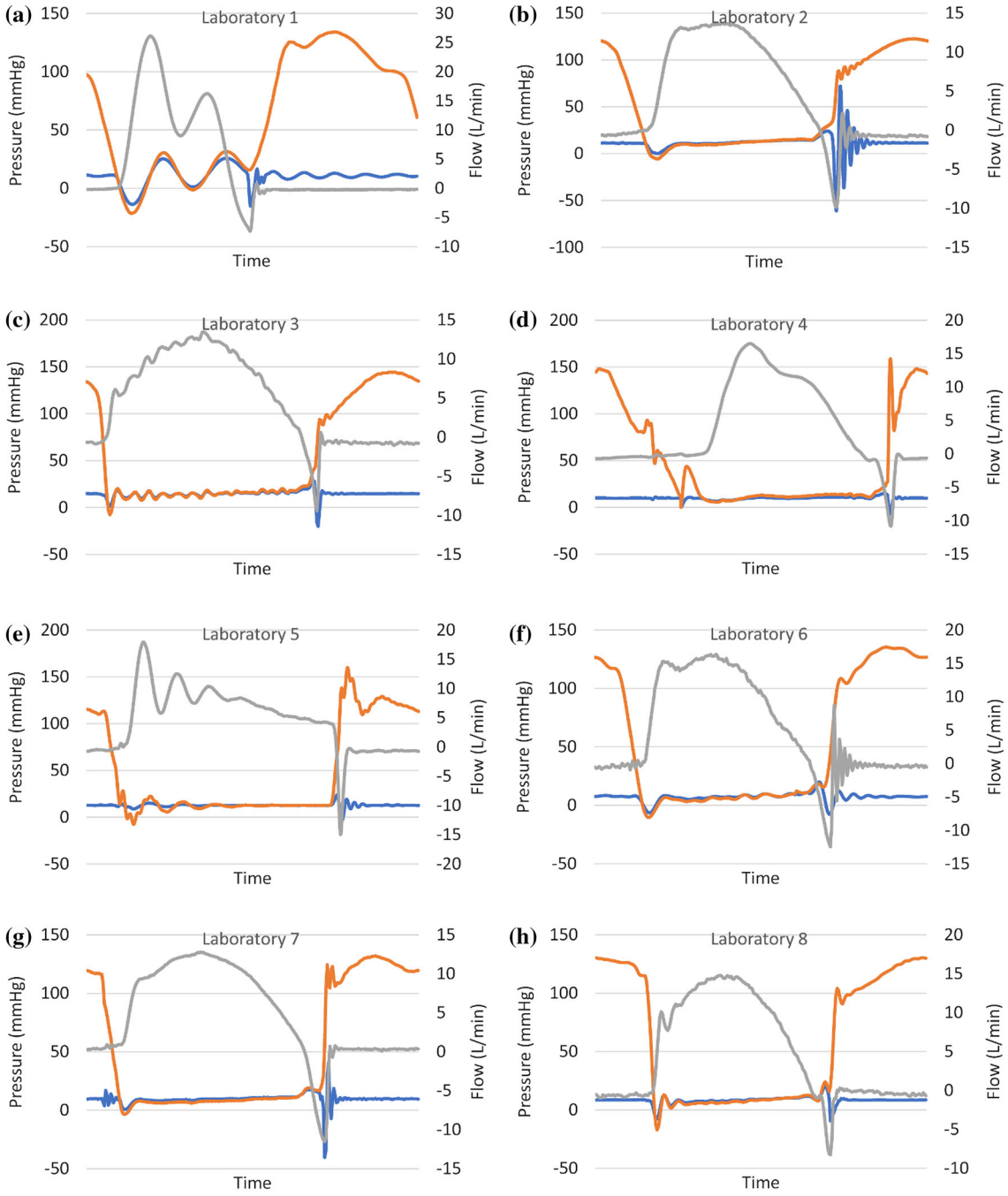

FIGURE B.4. Pressure and flow waveforms - mitral 31 mm. Curves shown are ventricular pressure (orange), atrial pressure (blue) and mitral flow (gray)

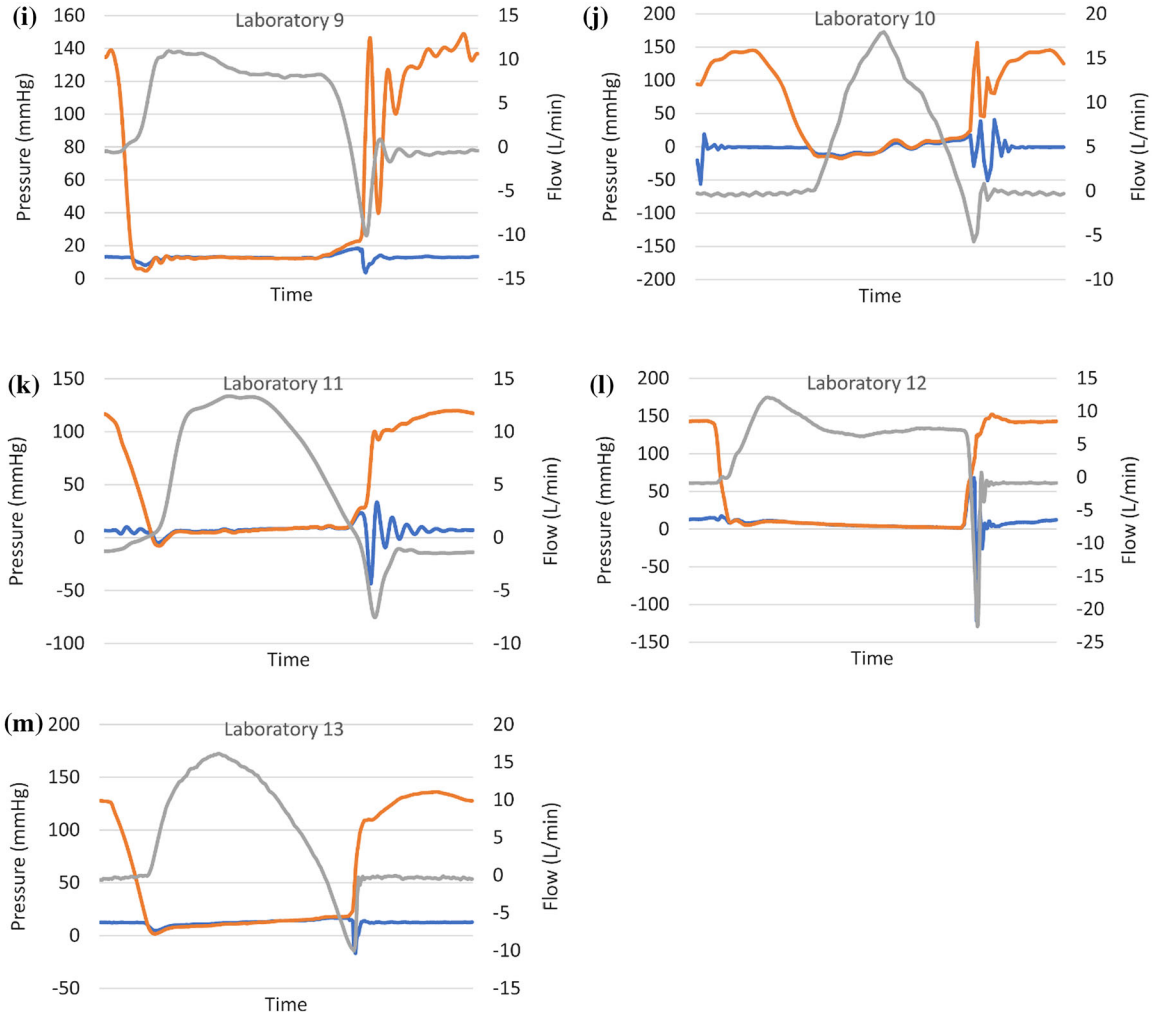

FIGURE B.4. continued

ACKNOWLEDGMENTS

We thank St. Jude Medical, Inc. (now part of Abbott) for providing the test valves. The findings and conclusions in this article have not been formally disseminated by the U.S. FDA and should not be construed to represent any agency determination or policy. The mention of commercial products, their sources, or their use in connection with material reported herein is not to be construed as either an actual or implied endorsement of such products by the U.S. Department of Health and Human Services.

FUNDING

The authors did not receive any funding to carry out the work.

DISCLAIMER

The mention of commercial products, their sources, or their use in connection with material reported herein is not to be construed as either an actual or implied endorsement of such products by the U.S. Department of Health and Human Services.

CONFLICT OF INTEREST

All authors declare that they have no conflicts of interest.

ETHICAL APPROVAL

This article does not contain any studies with human participants or animals performed by any of the authors.

INFORMED CONSENT

This article does not contain any studies with human participants.

REFERENCES

[1]Barbara, V., C. Daniele, M. Grigioni, A. Palombo, and A. Sargentini. In vitro evaluation of prosthetic heart valves: towards comparable testing. *J. Med. Eng. Technol.* 16:10–14, 1992.

[2]Barbaro, V., P. Bartolini, C. Daniele, M. Grigioni, and A. Palombo. Prosthetic heart valve evaluation in vitro: critical aspects of data comparability. *Int. J. Artif. Organs* 14:343–349, 1991.

[3]Cornhill, J. F. An aortic-left ventricular pulse duplicator used in testing prosthetic aortic heart valves. *J. Thorac. Cardiovasc. Surg.* 4:550–558, 1977.

[4]Davis K., J. H. Muller, C. J. Meyer, F. E. Smit. Evaluating the impact of air compliance chamber volumes on valve performance for three different heart valves. In: 2018 3rd Biennial South African Biomedical Engineering Conference (SAIBMEC), Stellenbosch, 2018, pp. 1–4.

[5]ISO 5840-3:2013: Cardiovascular Implants—Cardiac Valve Prostheses—Part 3: Heart Valve Substitutes Implanted by Transcatheter Techniques. International Organization for Standardization, Geneva, Switzerland.

[6]ISO 5840-2:2015. Cardiovascular Implants—Cardiac Valve Prostheses—Part 2: Surgically Implanted Heart Valve Substitutes. International Organization for Standardization, Geneva, Switzerland.

[7]Raghav, V., S. Sastry, and N. Saikrishnan. Experimental assessment of flow fields associated with heart valve prostheses using particle image velocimetry (PIV): recommendations for best practices. *Cardiovasc. Eng. Technol.* 9:273–287, 2018.

[8]Retta, S. M., J. Kepner, S. Marquez, B. A. Herman, M. C. S. Shu, and L. W. Grossman. In-vitro pulsatile flow measurement in prosthetic heart valves: an inter-laboratory comparison. *J. Heart Valve Dis.* 26:72–80, 2017.

[9]Robinson, R. A., R. F. Carey, and B. A. Herman. Evaluation of an in vitro cardiac pulse duplicator. *J. Clin. Eng.* 15:131–138, 1990.

[10]Schichl, K., and K. Affeld. A computer controlled versatile pulse duplicator for precision testing of artificial heart valves. *Int. J. Artif. Organs* 16:10, 1993.

[11]Wei, Z. A., S. J. Sonntag, M. Toma, S. Singh-Gryzbon, and W. Sun. Computational fluid dynamics assessment associated with transcatheter heart valve prostheses: a position paper of the ISO Working Group. *Cardiovasc. Eng. Technol.* 9:289–299, 2018.

[12]Yoganathan, A. P., W. H. Corcoran, and E. C. Harrison. Pressure drops across prosthetic aortic heart valves under steady and pulsatile flow—in vitro measurements. *J. Biomech.* 12:153–164, 1979.

Publisher's Note Springer Nature remains neutral with regard to jurisdictional claims in published maps and institutional affiliations.